5-HT3 receptor ion size selectivity is a property of the transmembrane channel, not the cytoplasmic vestibule portals

Nicole K. McKinnon,[1] David C. Reeves,[1] and Myles H. Akabas[1,2,3]

[1]Department of Physiology and Biophysics, [2]Department of Neuroscience, and [3]Department of Medicine, Albert Einstein College of Medicine of Yeshiva University, Bronx, NY 10461

5-HT3A receptors select among permeant ions based on size and charge. The membrane-associated (MA) helix lines the portals into the channel's cytoplasmic vestibule in the 4-Å resolution structure of the homologous acetylcholine receptor. 5-HT3A MA helix residues are important determinants of single-channel conductance. It is unknown whether the portals into the cytoplasmic vestibule also determine the size selectivity of permeant ions. We sought to determine whether the portals form the size selectivity filter. Recently, we showed that channels functioned when the entire 5-HT3A M3–M4 loop was replaced by the heptapeptide M3–M4 loop sequence from GLIC, a bacterial Cys-loop neurotransmitter gated ion channel homologue from *Gloebacter violaceus*. We used homomeric 5-HT3A receptors with either a wild-type (WT) M3–M4 loop or the chimeric heptapeptide (5-HT3A–glvM3M4) loop, i.e., with or without portals. In Na^+-containing buffer, the WT receptor current–voltage relationship was inwardly rectifying. In contrast, the 5-HT3A–glvM3M4 construct had a negative slope conductance region at voltages less than −80 mV. Glutamine substitution for the heptapeptide M3–M4 loop arginine eliminated the negative slope conductance region. We measured the relative permeabilities and conductances of a series of inorganic and organic cations ranging from 0.9 to 4.5 Å in radius (Li^+, Na^+, ammonium, methylammonium, ethanolammonium, 2-methylethanolammonium, dimethylammonium, diethanolammonium, tetramethylammonium, choline, tris [hydroxymethyl] aminomethane, and *N*-methyl-D-glucamine). Both constructs had measurable conductances with Li^+, ammonium, and methylammonium (size range of 0.9–1.8-Å radius). Many of the organic cations >2.4 Å acted as competitive antagonists complicating measurement of conductance ratios. Analysis of the permeability ratios by excluded volume theory indicates that the minimal pore radius for 5-HT3A and 5-HT3–glvM3M4 receptors was similar, ∼5 Å. We infer that the 5-HT3A size selectivity filter is located in the transmembrane channel and not in the portals into the cytoplasmic vestibule. Thus, the determinants of size selectivity and conductance are located in physically distinct regions of the channel protein.

INTRODUCTION

Cys-loop receptor neurotransmitter-gated ion channels, also referred to as pentameric ligand-gated ion channels (pLGICs), play a ubiquitous role in mediating fast synaptic neurotransmission. In mammals, the Cys-loop receptor superfamily includes receptors for serotonin (5-HT), acetylcholine (ACh), GABA, and glycine. All Cys-loop receptor superfamily subunits have a similar transmembrane topology. They have an ∼200–amino acid N-terminal extracellular ligand-binding domain and a similarly sized C-terminal domain with four (M1, M2, M3, and M4) transmembrane segments (Akabas, 2004; Lester et al., 2004; Changeux, 2010). Residues in the M2 segment line the transmembrane ion channel. The cytoplasmic loop between the M3 and M4 segments has the lowest degree of sequence conservation among subunits. The functions of the M3–M4 loop remain uncertain, although there is increasing evidence that the loop contributes to receptor assembly (Kracun et al., 2008), trafficking (Connolly, 2008), and conductance (Kelley et al., 2003; Deeb et al., 2007). In the 4-Å resolution structure of the homologous nicotinic ACh receptor, only the C-terminal portion of the M3–M4 loop, forming the MA helix, is sufficiently ordered to permit determination of its structure (Unwin, 2005). The five MA helices form an inverted pyramid that creates a water-filled vestibule at the cytoplasmic end of the channel (Fig. 1 A). Ions can move from the cytoplasm into the vestibule through portals or gaps between the MA helices.

A critical functional property for ion channels is their ability to conduct specific ions across the cell membrane. The pLGICs select permeant ions on the basis of both charge and size. It was assumed that the major determinants of selectivity and conductance were in the transmembrane channel itself. However, recent studies in the serotonin 5-HT3 receptors showed that residues in the cytoplasmic M3–M4 loop are important determinants

N.K. McKinnon and D.C. Reeves contributed equally to this paper.
Correspondence to Myles H. Akabas: myles.akabas@einstein.yu.edu

Abbreviations used in this paper: pLGIC, pentameric ligand-gated ion channel; WT, wild type.

The Rockefeller University Press $30.00
J. Gen. Physiol. Vol. 138 No. 4 453–466
www.jgp.org/cgi/doi/10.1085/jgp.201110686

of the single-channel conductance. Homomeric 5-HT3A receptors have a sub-picosiemen single-channel conductance, whereas heteromeric receptors containing 5-HT3A and 5-HT3B subunits have a single-channel conductance of ~16 pS (Davies et al., 1999). Mutating three arginine residues in the 5-HT3A M3–M4 loop to the corresponding residues in the 5-HT3B subunit results in channels with a conductance similar to the heteromeric receptors. These three arginines lie in the MA helix near the C terminus of the M3–M4 loop (Fig. 1 A, C, and D). They presumably line the portals that form the entrance to the cytoplasmic vestibule seen in the 4-Å resolution cryo-electron microscopic structure of the nicotinic ACh receptor (Fig. 1, C and D). Additionally, the introduction of arginine residues at MA helix positions −4′ or 0′ in neuronal ACh α4β2 receptor halved the single-channel conductance (Hales et al., 2006). It was surprising that residues in the portals to the cytoplasmic vestibule have such a significant impact on channel conductance. This raises the question of whether the portals into the cytoplasmic vestibule also play a significant role in forming the size selectivity filter that determines the size of the largest ion that can permeate through the receptor.

Until 2005, there were no known prokaryotic members of the pLGIC superfamily. Using iterative BLAST searches, prokaryotic members of the superfamily were identified (Tasneem et al., 2005). The bacterial homologues have weak amino acid sequence conservation with the eukaryotic family members and lack the canonical pair of disulfide-linked cysteines in the extracellular ligand-binding domain (Tasneem et al., 2005). Nevertheless, based on crystal structures, the prokaryotic homologues appear to share a similar domain structure with their eukaryotic counterparts (Brejc et al., 2001; Unwin, 2005; Hilf and Dutzler, 2008, 2009; Bocquet et al., 2009). One of these prokaryotic homologues from *Gloebacter violaceus*, GLIC, was shown to be a proton-gated cation-selective channel (Bocquet et al., 2007). The recent x-ray crystal structure of the *Caenorhabditis elegans* GluCl channel, a homomeric Cys-loop receptor homologue, does not provide any insight into the structure of the M3–M4 loop, because the loop was replaced by a tripeptide in the construct that was crystallized (Hibbs and Gouaux, 2011).

Notably, the bacterial channels lack the large intracellular loop between the third and fourth transmembrane helices (M3–M4 loop) that is present in all known eukaryotic subunits (Donizelli et al., 2006). Surprisingly, however, chimeric 5-HT3 or GABA ρ subunits, in which the heptapeptide predicted to form the M3–M4 loop in the GLIC channel replaced the endogenous M3–M4 loop, were fully functional when expressed heterologously (Jansen et al., 2008). In the chimeric 5-HT3 receptors with the GLIC heptapeptide loop, there is no cytoplasmic vestibule and thus no portals (Fig. 1, A and B). Ions pass from the cytoplasmic end of the channel directly into the cytoplasm.

Given the strong effect that the M3–M4 loop residues have on the single-channel conductance of cation-selective Cys-loop receptors, we hypothesized that the portals might also have a significant role in forming the size selectivity filter in these receptors. By measuring

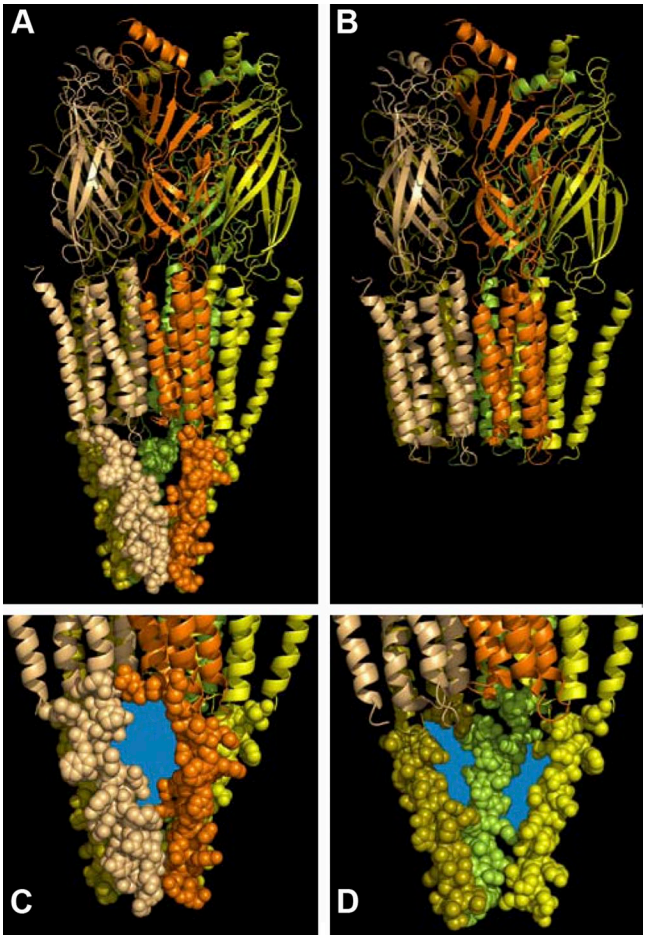

Figure 1. The MA-helix structure in the M3–M4 loop region and the portals into the channel's cytoplasmic vestibule using the 4-Å resolution cryo-EM nicotinic ACh receptor structure (Protein Data Bank accession no. 2BG9). Only the MA-helix portion of the M3–M4 loop region structure was resolved. (A) The entire receptor structure is shown, including the largely β-strand extracellular domain, the largely α-helical membrane-spanning domain, and the cytoplasmic MA helix. The first two domains are shown in ribbon cartoon representation, whereas the MA helix is shown in space-filling representation. Each subunit is shown in a different color for illustrative purposes. (B) The structure after removal of the cytoplasmic M3–M4 loop domain. (C) Close-up view from the cytoplasm of a portal into the channel's cytoplasmic vestibule. The portal region that ions would traverse to enter or leave the vestibule is colored blue. (D) View of the channel's cytoplasmic vestibule. The MA helices from the front two subunits (orange and tan) have been removed to visualize the cytoplasmic vestibule and the cytoplasmic mouth of the channel. The portals between the MA helices of the remaining three subunits are colored blue. Figure constructed with PyMOL version 1.4.1 and Photoshop version 10.0.1.

the permeability of a series of organic cations, the minimum channel diameter of 5-HT3A receptors was inferred to be ~7.6 Å (Yang, 1990). The 5-HT3A receptor construct with the truncated prokaryotic M3–M4 loop removes the cytoplasmic domain, allowing ions to exit directly from the cytoplasmic end of the channel into the cytoplasm without having to pass through the portals. This allowed us to test the role of the portals in determining the size selectivity for permeant ions. We concentrated on the 5-HT3 receptor for this study, as its ion-permeation properties have been extensively investigated (Reeves and Lummis, 2002; Peters et al., 2005; Barnes et al., 2009), and it readily functions as a recombinant homomer with or without its intracellular loop (Jansen et al., 2008). To determine the role of the M3–M4 loop in forming the size selectivity filter for permeant ions, we measured the relative permeabilities and conductances of a series of cations of increasing radius to obtain estimates for the minimum pore diameter of homomeric 5-HT3A receptors with either a wild-type (WT) or truncated M3–M4 loop, i.e., with or without the portals. The experiments indicate that the size selectivity filter is located in the transmembrane channel and not in the cytoplasmic vestibule portals.

MATERIALS AND METHODS

Mutagenesis and *Xenopus laevis* expression

Point mutations of the 5-HT3A–glvM3M4 receptor in the pXOON plasmid were generated using the QuikChange site-directed mutagenesis kit (Agilent Technologies). Successful incorporation of the mutation was verified by DNA sequencing of the entire coding region. The pXOON plasmid was linearized using NheI and capped mRNA prepared with the T7 RNA polymerase (mMessage mMachine; Invitrogen) as described previously (Jansen et al., 2008).

Oocytes were harvested from female *Xenopus* (Nasco Science). Oocytes were defolliculated by incubation in a solution containing 2 mg/ml Type 1A collagenase (Sigma-Aldrich) in OR2 (82.5 mM NaCl, 2 mM KCl, 1 mM $MgCl_2$, and 5 mM HEPES, with pH adjusted to 7.5 with NaOH) for 60 or 75 min at room temperature. Oocytes were washed in OR2 and stored at 16°C in SOS medium (82.5 mM NaCl, 2.5 mM KCl, 1 mM $MgCl_2$, 5 mM HEPES, pH 7.5, with 100 IU/ml penicillin, 100 µg/ml streptomycin, and 250 ng/ml amphotericin B; Invitrogen) and 5% horse serum (Sigma-Aldrich). 24 h after isolation, oocytes were injected with 23 nl (2.3 ng) mRNA and kept in horse serum media for 2–3 d at 16°C.

Electrophysiological recording

Currents were recorded from oocytes 3–5 d after injection, under two-electrode voltage clamp. Oocytes were continuously superfused under gravity application at 5 ml min^{-1} with Ca^{2+}-free frog Ringer's buffer (115 mM NaCl, 2.5 mM KCl, 1.8 mM $MgCl_2$, and 10 mM HEPES, pH 7.5 with NaOH), to which 5-HT was added as required. The perfusion chamber volume was 200 µl, and the ground electrode was connected to the bath by a 3-M KCl/agar bridge. The holding potential was maintained at −80 mV. Glass microelectrodes had a resistance of <2 MΩ when filled with 3 M KCl. Salts were purchased from Thermo Fisher Scientific or Sigma-Aldrich.

For the determination of size selectivity, oocytes expressing the 5-HT3A receptor were exposed to the reference solution (98 mM NaCl, 1 mM $MgCl_2$, 1 mM NaOH, and 5 mM HEPES, pH 7.4) either with or without 5-HT. Either saturating (50 µM 5-HT) or nonsaturating 5-HT concentrations were used. For the nonsaturating 5-HT concentration, an approximately EC_{30} 5-HT concentration (400–1,200 nM) was used. To determine the conductance and reversal potential, a ramp protocol was used to vary the holding potential three times from −120 to + 60 mV over 14 s (1 s per ramp). Control ramps were recorded before application of 5-HT. The oocytes were

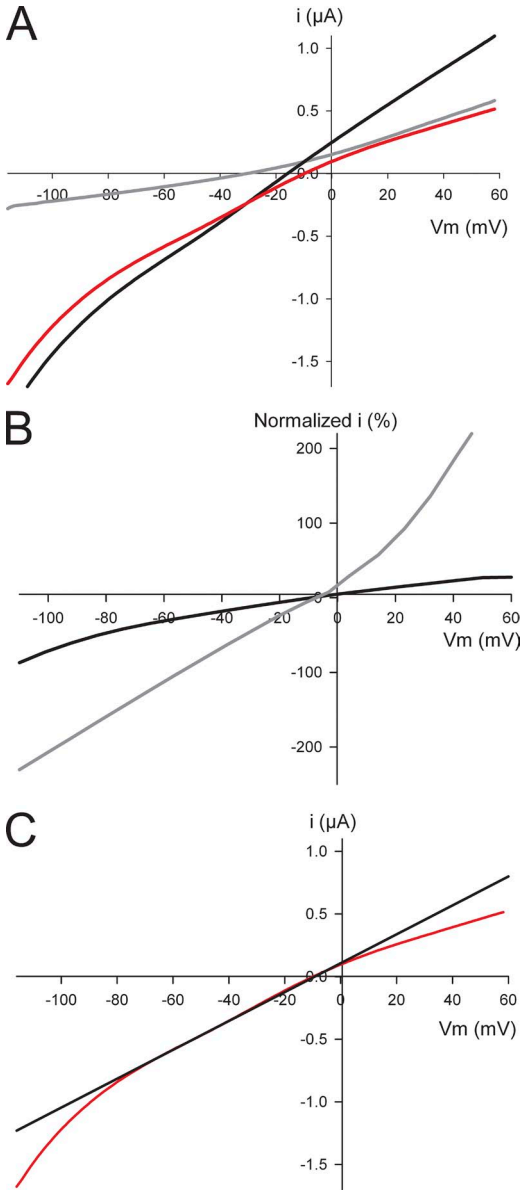

Figure 2. (A) I-V ramp (red) for a WT 5-HT3A receptor. Red curve is the background-subtracted I-V ramp of an oocyte expressing WT 5-HT3A receptor. It is the I-V ramp in the presence of 5-HT (black) minus a ramp in the absence of 5-HT (gray). (B) Normalized I-V ramps from a single oocyte at subsaturating (0.6 µM; black line) and saturating (10 µM; gray line) 5-HT concentrations. Both currents are normalized to the maximum current at −120 mV for the subsaturating 5-HT concentration (−1.8 µA). The maximum current for the saturating 5-HT concentration at −120 mV is −4.5 µA. (C) Tangent line (black) shown on the linear portion from −70 to −30 mV of a WT 5-HT3A I-V curve (red).

then perfused with 5-HT dissolved in the reference solution. Ramps were obtained after the current had reached a plateau. There was minimal desensitization (<5%) during the period in which the ramps were obtained. After a 4-min wash, to provide ample time for complete recovery from desensitization, the oocytes were exposed to the solutions containing the test cation (98 mM of test cation-Cl, 1 mM $MgCl_2$, 1 mM NaOH, and 5 mM HEPES, pH 7.4) in the absence or presence of nonsaturating 5-HT concentrations. Oocytes were perfused with the test cation solution for a period sufficient to ensure complete solution exchange before the ramps in the absence of 5-HT were obtained. The oocytes were then perfused with 5-HT in the test cation solution. Ramps were obtained after the current had reached a plateau. There was minimal desensitization (<5%) during the period in which the ramps were obtained. For all of the cations except NH_4^+, the internal oocyte ion concentrations did not change significantly. Ramps in Na^+-containing buffer immediately after the test cation solution were identical to the initial ramps in Na^+ solution before the test cation, except with NH_4^+, where there were changes in the ramp suggestive of changes in the internal oocyte ion composition, perhaps the pH. No correction was made in the reversal potential calculations for the presence of 1 mM Mg^{2+} in all of the solutions.

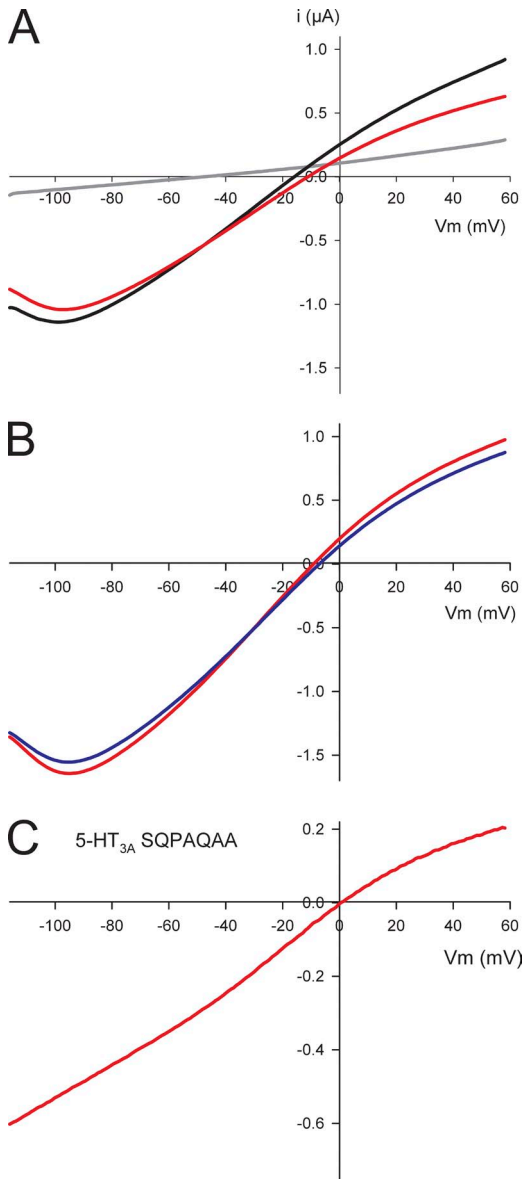

Figure 3. Characterization of the negative slope conductance of the 5-HT3A–glvM3M4 receptor. (A) I-V ramp (red) for a 5-HT3A–glvM3M4 receptor demonstrating the negative slope conductance at the more negative voltages. Red curve is the background-subtracted I-V ramp of an oocyte expressing 5-HT3A–glvM3M4 receptor. It is the I-V ramp in the presence of 5-HT (black) minus a ramp in the absence of 5-HT (gray). All other I-V curves shown are the background-subtracted curves. (B) I-V curves for a 5-HT3A–glvM3M4 receptor in the presence of 1 mM EGTA (blue) and the absence of EGTA (red). (C) I-V curve for the 5-HT3A–SQPAQAA. The negative slope conductance is not present when the Arg residue is removed from the M3–M4 loop. A 5-HT EC_{30} concentration (400–1,200 nM) was used for the experiments and determined for each oocyte expressing 5-HT3A receptors.

Calculation of conductance ratios

Conductance ratios for the various cations were determined by calculating the slope for each solution using the linear portion of I-V curve from test voltages of −70 through −30 mV (Fig. 2 C), and normalizing to the Na^+ test solution conductance. Each oocyte was tested in the presence of both the reference solution and the test solution; therefore, each test cation was normalized to the Na^+ reference conductance directly preceding it. Mean conductance ratios were calculating by pooling the data from at minimum three oocytes, using oocytes from at least two different animals. Unpaired two-tailed *t* tests (PRISM 5.0; GraphPad Software) were used to establish significant differences.

Calculation of reversal potentials

For each test solution, the mean current recorded from three sweeps in the absence of 5-HT was subtracted from the mean current in the presence of 5-HT to give the difference current $I_{5\text{-HT}}$ over the full voltage range (Fig. 2 A). The reversal potential V_r was determined by interpolating the plot of $I_{5\text{HT}}$ versus V at 0 mV. Mean reversal potentials were calculated by pooling the data from at least three independent experiments per test cation, using oocytes from at least two different animals. We used a one-way ANOVA test (PRISM 5.0; GraphPad Software) to establish any significant differences in reversal potentials obtained for the two 5-HT3A receptor constructs, with and without the large cytoplasmic M3–M4 domain, studied.

A modified Goldman-Hodgkin-Katz equation was used to calculate values for relative permeability (Cohen et al., 1992). For a test cation, X^+, the relative permeability P_x/P_{Na} was given by:

$$P_x / P_{Na} = \{[Na^+]_r \exp(\Delta VF / RT) - [Na^+]_t\} / [X]_t, \qquad (1)$$

where $\Delta V = V_t - V_r$ is the difference in the reversal potentials with the test cation; reference Na^+ solutions $[Na^+]_r$ and $[Na^+]_t$ are the concentrations of sodium in the reference and test solutions, respectively; and R, T, and F have their usual meanings. The reference solution contained 98 mM Na^+, 1 mM $MgCl_2$, 1 mM NaOH, and 5 mM HEPES, pH 7.4. No correction was made for the presence of 1 mM Mg^{2+} in the extracellular media. The extracellular Na^+ concentration was 1 mM in the test cation solution.

Estimation of the diameter of the 5-HT3 receptor pore at its narrowest point

Using the assumption that each cation X^+ is a sphere of diameter R_X, and that the pore at its narrowest point may be approximated by a cylinder with a narrow region of radius R_C, we applied excluded volume theory (Dwyer et al., 1980; Cohen et al., 1992) to estimate the smallest diameter of the 5-HT3 receptor pore. The relationship between relative permeability and radius can be given thus (from Cohen et al., 1992):

$$\sqrt{\frac{P_X}{P_{Na}}} = a - b*R_X,$$

where $a = R_C/(R_C - R_{Na})$, and $b = 1/(R_C - R_{Na})$.

We plotted the square root of the calculated permeability ratios P_X/P_{Na} versus ionic radius R_X and obtained the slope b and intercept a by linear regression. The diameter of the narrowest region of the pore is given by 2a/b. Ionic radii are taken from Cohen et al. (1992).

RESULTS

Mouse 5-HT3A receptors in *Xenopus* oocytes have an inwardly rectifying I-V relationship

We recorded the current passed in response to a ramp voltage protocol in oocytes expressing homomeric WT 5-HT3A receptors (Fig. 2 A). With Na^+ as the major charge carrier, the currents induced by submaximal 5-HT concentrations displayed inward rectification (Fig. 2 B, black line). This is consistent with previous studies of human, rat (Jones and Surprenant, 1994), and recombinant mouse 5-HT3 receptors (Hussy et al., 1994). In contrast, at saturating 5-HT concentrations (>10 µM), the I-V relationship became linear for WT 5-HT3A receptors (Fig. 2 B, gray line). Previous studies using mouse WT 5-HT3A expressed in *Xenopus* oocytes have also reported a lack of inward rectification (Maricq et al., 1991; Jansen et al., 2008). This change from inwardly rectifying to linear I-V relationship may be explained by the large currents (>5 µA) induced by a saturating concentration of 5-HT. As the currents become very large, the series access resistance becomes the limiting resistance rather than the membrane resistance of the 5-HT3A channels (Fig. 2 B), resulting in the linear I-V relationship.

GLIC chimeric M3–M4 loop alters the I-V relationship

In oocytes expressing the 5-HT3A–glvM3M4 receptor, the ramp currents recorded with Na^+ as the major charge carrier displayed a negative slope conductance at voltages below −80 mV that was not present with WT 5-HT3A (Fig. 3 A). A distinguishing feature of the native central nervous system 5-HT3A I-V relationship is a region of negative slope conductance reflecting a voltage-dependent block by external Ca^{2+} ions (Van Hooft and Wadman, 2003). However, with the 5-HT3A–glvM3M4 receptor, inclusion of 1 mM EGTA in the external bath solution did not significantly alter the negative slope

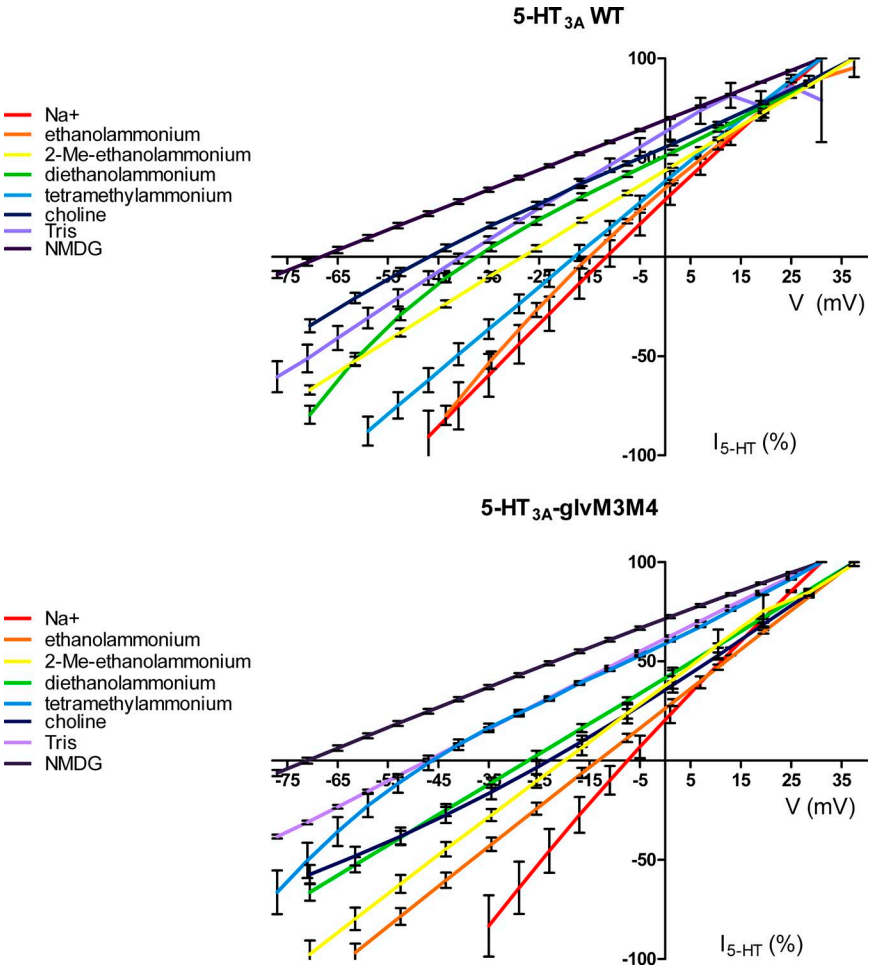

Figure 4. The effect of substitution of Na^+ with organic cations on the I-V relationship of 5-HT3 receptors at saturating concentrations of 5-HT (50 µM). (Top) 5-HT3A WT receptors. (Bottom) Chimeric 5-HT3A–glvM3M4 receptors. Data points at each potential sample are plotted as the mean normalized current ± SEM along with the interpolated fit through the points. The data were normalized for clarity to the current at either +31 or +37 mV, dependent on the exact protocol used.

conductance (Fig. 3 B). A recent study reported that an interaction of ATP and other cytoplasmic phosphates with arginine residues in the intracellular loop of 5-HT3 receptors contributes to the voltage-dependent Ca^{2+} block (Noam et al., 2008). To determine if the positively charged arginine residue in the heptapeptide loop played a role in the observed negative slope conductance, we replaced it with an uncharged glutamine (5-HT3A–SQPAQAA). The I-V relationship for this construct was similar to that observed for WT 5-HT3A and lacked the negative slope conductance at voltages more negative than −80 mV (Fig. 3 C). This suggests that the negative slope conductance arose from interactions between the heptapeptide M3–M4 loop arginine and cytoplasmic anions. It also suggests that cytoplasmic anions may be able to interact with the transmembrane electric field in the cytoplasmic mouth of the channel.

Replacement of extracellular Na^+ alters the I-V relationship of 5-HT3A receptors

To determine whether the 5-HT3A channel size selectivity filter is in the transmembrane channel or in the portals into the cytoplasmic vestibule, we measured the permeability relative to Na^+ of a series of inorganic and organic cations of increasing ionic radius in 5-HT3A channels with (WT 5-HT3A) and without (5-HT3A–glvM3M4) the large cytoplasmic domain (Fig. 4 and Table I). For the majority of replacement cations tested, the application of a saturating concentration of 5-HT (50 µM) induced robust currents over a wide range of holding potentials, allowing the measurement of a reversal potential for each cation (Fig. 4 and Table I). However, when extracellular Na^+ was replaced by several large cations (diameter of ≥9 Å), including tetraethylammonium, tetrapropylammonium, tetrabutylammonium, tetrahexylammonium, or L-arginine, no significant 5-HT–induced currents were observed with either WT or 5-HT3A–glvM3M4 constructs. In control extracellular solutions where Na^+ was omitted (98 mM sucrose), robust 5-HT–dependent currents were observed (more than 1.3 µA at +30-mV holding potential), which reversed at negative potentials (below −50 mV; Table I), consistent with the absence of a permeant extracellular charge carrier. We infer that the larger organic cations

TABLE I

Conductance and permeability ratios for various monovalent cations in WT and chimeric M3–M4 loop 5-HT3A receptors

Test cation	Radius	M3–M4 loop[a]	g_X/g_{Na}	±SEM	Vr ± SEM	V_X-V_{Na}	P_X/P_{Na}	*n*
	Å[b]				*mV*			
Lithium	0.9	+	0.3	0.05	−11.6 ± 2.4	0.6	1.01	4
		−	0.15	0.03	−4.1 ± 2.9	3.6	1.14	4
Sodium	1.0	+	1		−12.2 ± 3.0	0	1.00	4
		−	1		−7.7 ± 2.3	0	1.00	4
Ammonium	1.7	+	0.4	0.1	−11.4 ± 8.1[c]	0.8	1.02	4
		−	0.3	0.1	10.9 ± 2.6[c]	18.6	2.07	4
Methylammonium	1.8	+	0.14	0.09	−4.5 ± 1.8	7.7	1.35	5
		−	0.14	0.04	−8.7 ± 0.8	−1.0	0.95	4
Ethanolammonium	2.4	+	0.05	0.01	−14.9 ± 0.7	−2.7	0.89	5
		−	−0.01	0.02	−13.3 ± 1.2	−5.6	0.79	4
2-Methylethanolammonium	2.6	+	−0.003	0.05	−28.3 ± 1.0	−16.1	0.52	4
		−	0.07	0.06	−19.7 ± 1.7	−12.0	0.61	4
Dimethylammonium	2.6	+	−0.02	0.01	−25.7 ± 2.4	−13.5	0.58	3
		−	0.06	0.01	−24.2 ± 1.3	−16.5	0.51	4
Diethanolammonium	2.8	+	0.01	0.01	−36.7 ± 1.2	−24.5	0.37	3
		−	0.04	0.02	−27.2 ± 1.6	−19.5	0.45	4
Tetramethylammonium	2.9	+	0.01	0.01	−18.0 ± 1.8[c]	−5.8	0.78	4
		−	−0.01	0.01	−46.2 ± 2.3[c]	−38.5	0.21	4
Choline	3.2	+	−0.01	0.01	−46.7 ± 1.5[c]	−34.5	0.25	4
		−	0.01	0.01	−23.6 ± 2.2[c]	−15.9	0.52	4
Tris	3.3	+	0.04	0.04	−40.7 ± 1.4	−28.5	0.31	4
		−	0.06	0.05	−46.4 ± 0.1	−38.7	0.21	4
NMDG	4.5	+	0.10	0.10	−68.6 ± 1.7	−56.4	0.10	4
		−	0.15	0.10	−70.7 ± 1.2	−63.0	0.07	4
Sucrose		+			−63.8 ± 1.8	−51.6	0.12	3
		−			−69.5 ± 2.3	−61.8	0.08	4

[a]M3–M4 loop: +, WT loop; −, glvM3M4 loop.
[b]Ionic radii from Cohen et al. (1992).
[c]A significant difference ($P < 0.05$) between reversal potential for WT and glvM3M4 loop by one-way ANOVA.

inhibited the 5-HT3 receptor at the extracellular concentration used (98 mM).

In the case of tetrahexylammonium, as little as 500 μM was required to completely inhibit 5-HT–induced currents. The block did not appear to be voltage dependent, as no 5-HT–specific currents were observed over the entire range of potentials tested (−120 to +60 mV). Millimolar concentrations of tetraethylammonium were previously shown to inhibit 5-HT3 receptor function by competing for the 5-HT–binding site (Kooyman et al., 1993), and as the entire tetraalkylammonium series tested, except tetramethylammonium, also appeared to cause inhibition in our hands, we did not include them in our size selectivity experiments.

Removal of the M3–M4 loop alters the permeability ratios for a subset of permeant cations

For both 5-HT3A WT and 5-HT3A–glvM3M4 receptors, we calculated the shift in reversal potential (ΔV_r) for each test cation by subtracting the measured reversal potential obtained in Na^+ in that receptor from that obtained using each test cation (Fig. 4 and Table I). For 8 of the 11 test cations, there was no significant difference in the shift in reversal potential when comparing 5-HT3A WT and 5-HT3A–glvM3M4 receptors. The reversal potential shift on removal of the loop was, however, significantly different for three of the test cations (two-way ANOVA; $P < 0.05$; Fig. 5, top). The shift was to more positive potentials for ammonium and choline, and to a more negative potential for tetramethylammonium.

Conductance ratios and the 5-HT3A M3–M4 loop

Several factors complicated attempts to measure the conductance ratios for the various organic cations. As noted above, we discovered that under the expression conditions that we used, the level of expression of both 5-HT3A receptor constructs was so high that at maximal activation by saturating 5-HT concentrations, the series

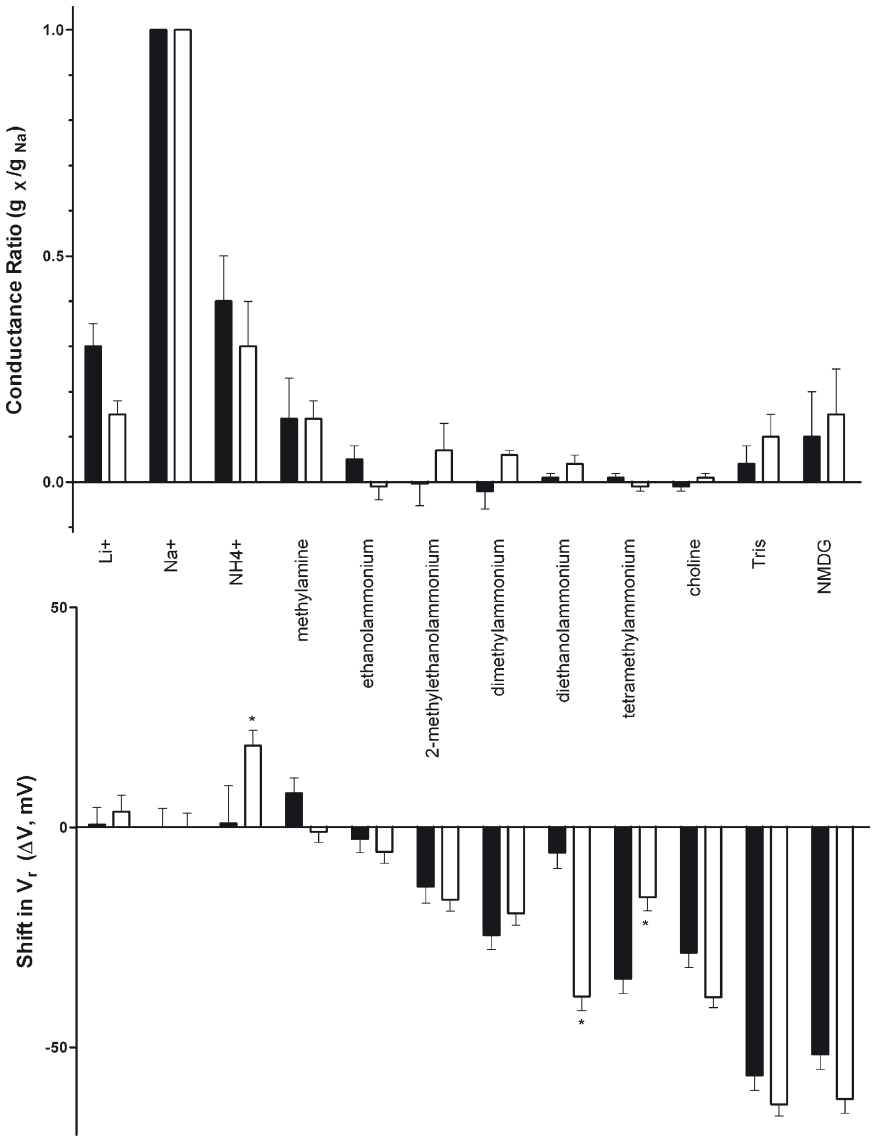

Figure 5. Shifts in the reversal potential of $I_{5\text{-HT}}$ and changes in relative conductance upon substitution of Na^+ with inorganic and organic cations in oocytes expressing either 5-HT3A WT (filled bars) or chimeric 5-HT3A–glvM3M4 (open bars) receptors. (Top) Conductance ratios were calculated taking the slope across the voltage range of −70 to −30 mV for each cation and dividing by the Na^+ slope. (Bottom) Reversal potentials derived from the data in Table I were subtracted from those determined in 98 mM Na^+ for each subunit. Where a significant difference in ΔV_r was observed between the two receptors tested, it is marked with an asterisk (*, $P < 0.01$; two way ANOVA).

resistance was the limiting resistance. This led to linear I-V relationships for most of the cations studied (not depicted). For the majority of replacement cations tested, the application of a nonsaturating concentration of 5-HT did not induce significant currents over the tested voltage range (−120 to +60 mV; Figs. 6 and 7, and Table I). Surprisingly, even at positive potentials where the expected outward current would be carried by internal K^+ ions, no significant currents were observed (Figs. 6 and 7). This implied that the substituted cations either blocked the channel or acted as competitive antagonists at the 5-HT–binding sites, or both. For WT receptors, the 5-HT concentration–response relationship was shifted to the right in extracellular ethanolammonium

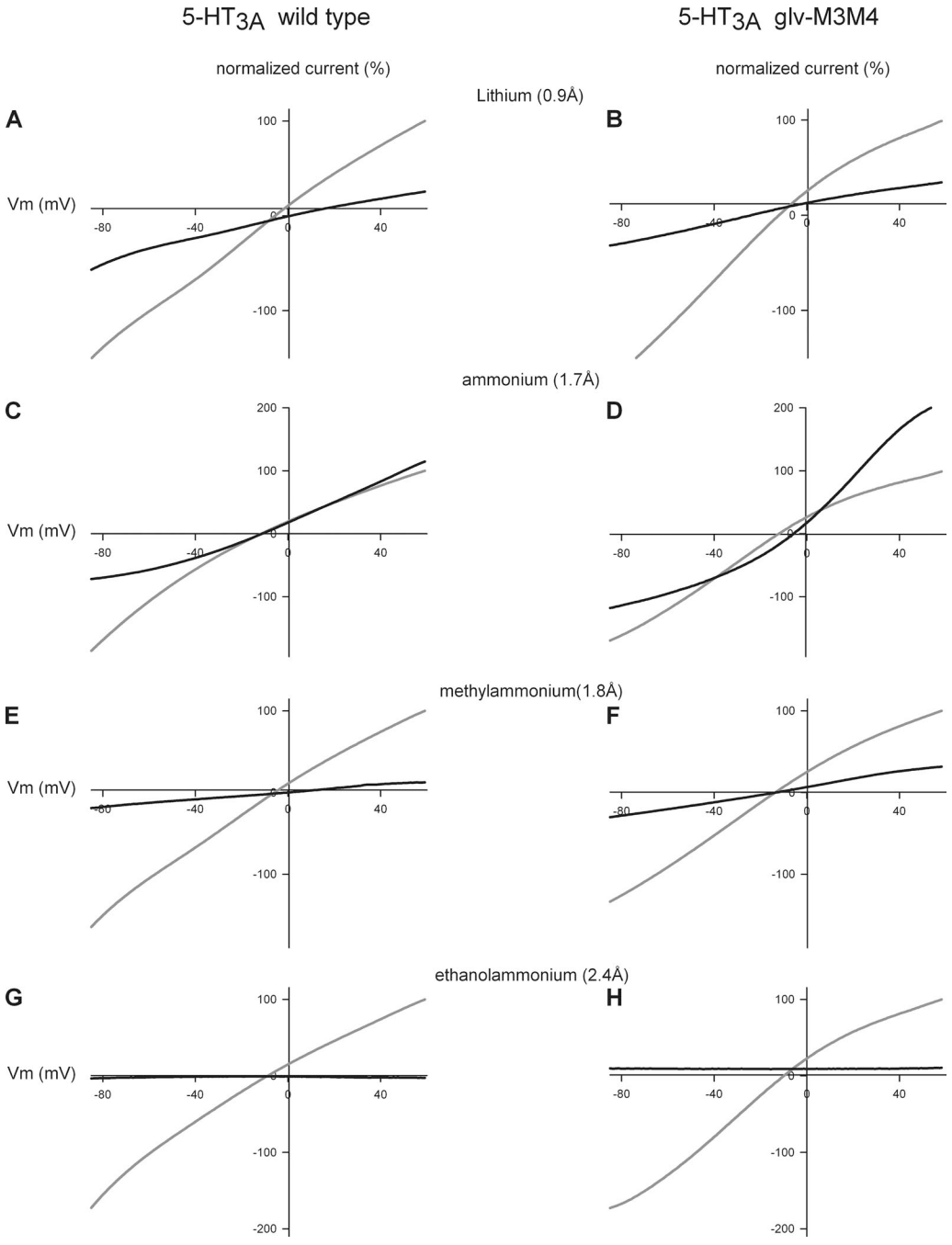

Figure 6. Comparison of the I-V relationship of the WT 5HT3A and chimeric 5-HT3A–glvM3M4 receptor in cations ≥2.4-Å radius. Normalized I-V relationships for WT 5-HT3A in external 98 mM of Na^+ solution (gray) or external 98 mM of cation solution (black). (A, C, E, and G) WT 5HT3A and (B, D, F, and H) 5-HT3A–glvM3M4 receptors. (A and B) Li^+, (C and D) NH_4^+, (E and F) methylammonium, and (G and H) ethanolammonium. Both receptors are permeant to cations of <2.4 Å. Subsaturating concentrations of 5-HT were used in these experiments.

compared with extracellular Na^+. The 5-HT EC_{50} values were 0.8 ± 0.02 μM and 2.4 ± 0.6 μM in Na^+ and ethanolamine, respectively (not depicted). This suggested that at least some of the midsized cations were acting as competitive antagonists. Thus, at a given submaximal 5-HT concentration, the level of channel activation was different in Na^+-containing solutions as compared with solutions containing the test cation. Thus, differences in the measured slope conductances in Na^+ and some other cations were not arising from comparable levels of channel activation. This meant it was not possible to determine the conductance ratios for these cations.

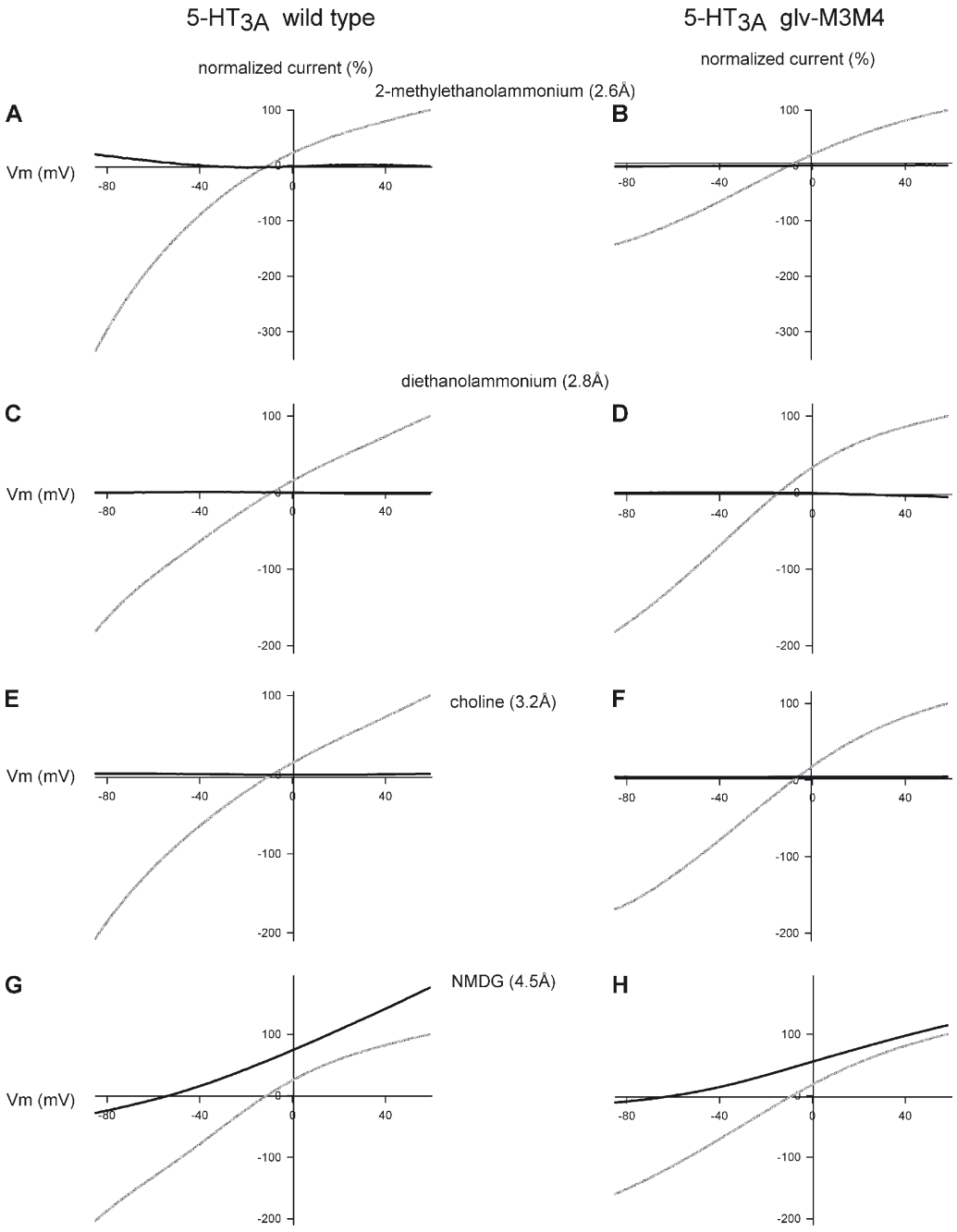

Figure 7. Comparison of I-V relationships for WT 5-HT3A and chimeric 5-HT3A–glvM3M4 receptors for cations between 2.6 and 4.5–Å radius. Normalized I-V relationship for WT 5-HT3A in external 98 mM of Na^+ solution (gray) or external 98 mM of cation solution (black). (A, C, E, and G) WT 5HT3A and (B, D, F, and H) 5-HT3A–glvM3M4 receptors. (A and B) 2-Methylethanolammonium, (C and D) diethanolammonium, (E and F) choline, and (G and H) NMDG. Neither receptor is significantly permeable to cations of >4.5-Å radius. The midsized cations (between 2.6 and 4.5 Å) had flat I-V relationships, possibly from the cation blocking the pore or from the cation acting as competitive antagonists at the 5-HT–binding site. Subsaturating concentrations of 5-HT were used in these experiments.

When extracellular Na^+ was replaced by several small cations (diameter of ≤2.4 Å), including lithium, ammonium, and methylammonium, significant 5-HT–induced currents were observed (Fig. 6). The inward rectification observed in the presence of extracellular Na^+ was absent for both the 5-HT3A WT and 5-HT3A–glvM3M4 receptors when the extracellular Na^+ was replaced with either lithium or methylammonium. We inferred that these three cations did not appear to cause significant competitive inhibition or channel block. For these cations, we measured the slope conductance for both the WT and 5-HT3A–glvM3M4–truncated receptor by taking the slope from the linear range of the I-V relationship across the voltage range of −70 to −30 mV (Fig. 2 C). We calculated conductance ratios (g_X/g_{Na}) for each test cation by normalizing the slope of the test cation from −70 to −30 mV to the slope of the reference Na^+ solution for the same voltages. For the cations tested, there was no significant difference in the conductance ratios calculated when comparing WT and truncated receptors (Table I and Fig. 5, bottom).

When NMDG (4.5 Å) was the major extracellular charge carrier, small 5-HT–induced currents were observed at positive voltages greater than the reversal potential, consistent with the efflux of potassium out of the cell, down its electrochemical gradient. This indicated that the 5-HT3A receptors were being activated under these ionic conditions. With NMDG as the test cation, a conductance ratio of <0.15 was calculated for both the WT and truncated receptor. This resulted from a small 5-HT–induced current observed at voltages more negative than the reversal potential (Fig. 6, G and H). The inward portion of the NMDG current was similar in magnitude to the current recorded with sucrose replacing the NaCl. Thus, we infer that this current was carried by the low concentrations of Na^+, Mg^{2+}, or other cation contaminants present in the extracellular solution and not by the NMDG.

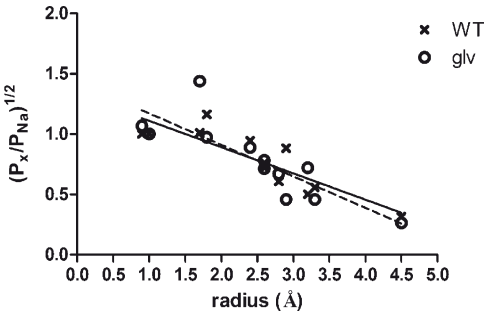

Figure 8. The relationship between relative permeability and ionic radius in 5-HT3 receptors. Plot of the square root of the relative permeability against ionic radius for the series of cations in Table I, along with linear regression lines for each dataset: solid line, WT; dashed line, 5-HT3A–glvM3M4. Note that two cations share the same calculated radius at 2.6 Å, and that the measured relative permeabilities are similar. NMDG, which was impermeant, was excluded from the linear regression analysis. The ammonium results were also excluded because of the large difference between the two channels and the confounding effects of ammonium ion substitution on the oocyte endogenous currents.

Estimation of the minimum pore diameter of 5-HT3A receptors

We used the measured reversal potentials of each receptor to calculate an estimate for the permeability of each test cation X^+ relative to that of Na^+ (P_X/P_{Na}; Table I). When relative permeability is plotted against ionic radius (Fig. 8), a negative correlation was found, with an overall pattern consistent with previous studies of the related nicotinic acetylcholine receptor (Cohen et al., 1992).

We applied excluded volume theory to obtain an estimate of the minimum pore diameter of each receptor by plotting the square root of the calculated relative permeability P_X/P_{Na} against ionic radius for the alkylammonium cations (Fig. 8). A linear regression provided values of y intercept, a, and slope, b, for 5-HT3A WT receptors (a = 1.44, and b = −0.27) and 5-HT3A–glvM3M4 receptors (a = 1.53, and b = −0.31). The R^2 values for the linear regression fits were 0.75 and 0.70 for 5-HT3A WT and 5-HT3A–glvM3M4 receptors, respectively. We therefore estimate that minimum pore diameters for 5-HT3A WT and 5-HT3A–glvM3M4 as 10.7 and 9.9 Å, respectively. The value of (a-1)/b should equal R_{Na}, and the respective values obtained, 1.6 and 1.7 Å, were found to be a reasonable approximation of the hydrated radius of Na^+ ions in solution (2.15 Å; Cohen et al., 1992).

DISCUSSION

The structure of Cys-loop receptor channels determines their functional conduction properties, such as (a) the conductance, i.e., the rate of ion translocation; (b) the ion selectivity (i.e., cation vs. anion, or K^+ vs. Na^+, etc.); and (c) the size of the largest permeant ion. The size selectivity filter is presumably the region in the open ion translocation pathway between the extracellular solution and the cytoplasm that has the minimum diameter. To understand how the Cys-loop receptor structure determines the functional properties, it is important to determine the location of the size selectivity filter. In the 5-HT3 receptors, residues in the MA helix near the C terminus of the cytoplasmic M3–M4 loop have a major impact on single-channel conductance (Kelley et al., 2003; Hales et al., 2006; Deeb et al., 2007; Carland et al., 2009). These residues may line the putative portals into the cytoplasmic vestibule (Fig. 1) (Unwin, 2005). This raised the question of whether residues in the M3–M4 loop also formed the size selectivity filter of the channel. In this work, we sought to determine whether the size selectivity filter was in the 5-HT3A cytoplasmic M3–M4 loop or in the transmembrane channel.

We measured the reversal potentials and conductance of cations with a range of sizes in both 5-HT3A WT and 5-HT3A–glvM3M4 chimeric receptors. As is apparent from Table I and Figs. 2, 3, and 4, for 8 of the 11 test cations, we found no significant difference in reversal potential when the WT cytoplasmic loop is replaced by the GLIC heptapeptide. The trend toward decreasing permeability with increasing ionic radius is similar to that previously found for nicotinic acetylcholine receptors (Cohen et al., 1992) and 5-HT3 receptors (Yakel et al., 1990; Yang, 1990, 1992). This indicates that the size selectivity filter is likely to operate by a simple steric sieve mechanism, consistent with the assumptions of excluded volume theory (Dwyer et al., 1980). Our results indicate that the ion size selectivity of 5-HT3A receptors with or without the WT M3–M4 large cytoplasmic loop is similar (Fig. 8 and Table I) and so is the predicted minimum channel diameter (Fig. 8). We therefore infer that in the open state, the putative portals of the 5-HT3 receptor cytoplasmic domain are larger than the minimum transmembrane pore diameter. The narrow region of the pore must be within the transmembrane channel region. We also infer that the size of the narrow region of the pore is not affected significantly by the presence or absence of the cytoplasmic domain, and that this dimension is likely an intrinsic property of the transmembrane region for each type of Cys-loop receptor.

Several lines of evidence suggest that the narrowest portion of the transmembrane channel is near the cytoplasmic end of M2. Mutation to cysteine of the 5-HT3A M2–2′ residue induces the formation of a high affinity Cd^{2+}-binding site at that level in the pore (Panicker et al., 2004). This suggests that this is a narrow region in the pore. Consistent with this, mutation of the 2′ position in nicotinic acetylcholine receptors significantly alters the relative permeabilities of small ions (Villarroel et al., 1991) and organic cations (Cohen et al., 1992). Experiments in our laboratory have shown previously that the most cytoplasmic two-helical turns of the pore-lining M2 helix (−2′ to 6′) are more rigid and tightly packed than the extracellular continuation of the M2 helix (Horenstein et al., 2001; Bera et al., 2002; Goren et al., 2004). Furthermore, in the $GABA_A$ receptor, we showed that picrotoxin, a rigid molecule that is roughly 9 Å in diameter, binds in the vicinity of the 2′ residue (Xu et al., 1995; Bali and Akabas, 2007). This implies that the channel narrows toward the cytoplasmic end; however, it did not preclude the possibility that the ion translocation pathway is even narrower in the portals of the cytoplasmic vestibule. The inhibition of 5-HT3 receptors by picrotoxin has been shown to depend on residues at the 6′ level (Das and Dillon, 2005). In addition, considerable evidence suggests that the charge selectivity filter is located near the cytoplasmic end of the transmembrane channel (Akabas et al., 1992; Galzi et al., 1992; Xu and Akabas, 1996; Reeves et al., 2001; Keramidas et al., 2004). Thus, we suggest that the cytoplasmic end of the transmembrane channel is the most likely location for the size selectivity filter measured in this work. Further mutational analysis of this region of the pore with concomitant measurement of minimum pore diameters will be required to locate precisely the size selectivity filter of 5-HT3 receptors.

Our results suggest that the size selectivity filter is located in a defined region within the transmembrane channel region. In contrast, determinants of single conductance appear to be distributed along the entire ion-conducting pathway. The charged residues at the extracellular, intermediate, and cytoplasmic rings of charge have significant impacts on single-channel conductance (Imoto et al., 1988). Evidence has been presented that residues in the extracellular vestibule can affect conductance (Hansen et al., 2008) as well as residues in the portals into the cytoplasmic vestibule (Kelley et al., 2003; Hales et al., 2006). Thus, determinants of single-channel conductance are more broadly distributed. This suggests that the sterically narrowest region that determines size selectivity does not also form the major determinant of single-channel conductance. In the 5-HT3A receptor, the major determinant of single-channel conductance appears to be in the three arginine residues in the cytoplasmic MA helix that are hypothesized to line the portals into the cytoplasmic vestibule of the channel (Kelley et al., 2003). Our results demonstrate that this region does not form the size selectivity filter.

As was mentioned in the Results section, attempts to measure the conductance ratios of the various cations in this study were complicated by inhibitory effects of extracellular Na^+ replacement. We observed a strong inhibition by midsized cations (2.4–3.3 Å) and also by most of the tetraalkylammonium cations (∼9–17-Å diameter). The I-V relationships with these ions lacked voltage dependence, suggesting that the inhibition was not a result of channel block. Consistent with this, we showed that ethanolammonium behaved as a competitive antagonist causing a right shift in the 5-HT concentration–response relationship. It should be noted that in these experiments, these cations were present at a concentration of 100 mM, orders of magnitude higher than the agonist concentration. Thus, at best they are very weak competitive antagonists. Tetraethylammonium was previously shown to inhibit 5-HT3 receptor function by competing for the 5-HT–binding site (Kooyman et al., 1993). This suggests that the large tetraalkylammonium ions may inhibit by binding to the receptor at a site not located in the pore, and therefore they cannot give information on the pore diameter. For several small cations including lithium, ammonium, and methylammonium that did not appear to inhibit, we found no significant difference in the conductance ratios

for the tested cations between the 5-HT3A WT and 5-HT3A–glvM3M4–truncated receptor. Because of the methodological problems, we did not pursue further characterization of the conductance ratios.

Interestingly, we did detect a greater than twofold difference in permeability ratios for three of the test cations (Table I). Ammonium and choline were more permeable through 5-HT3A–glvM3M4 channels, and tetramethylammonium was more permeable through the WT channel. Because the changes were not consistent between channels with and without the M3–M4 loop, and because for the entire set of cations excluded volume analysis suggests that the channel diameters are similar, we do not understand the basis for the changes observed with these three cations. Although ammonium and tetramethylammonium are relatively spherical in shape, choline is not. So the basis of the differential effects on permeability does not appear to depend on molecular shape of the cations. It is possible that removal of the WT M3–M4 loop caused small structural changes in the shape of the narrow region of the transmembrane channel, but the basis for the differential effects is not obvious. Alternatively, the effects may be the result of interactions, perhaps electrostatic, with parts of the cytoplasmic domain, such as the MA helix (Hales et al., 2006). This, however, would suggest that the measured permeabilities of different ions represent a summation of interaction effects with different regions of the channel. The strength of these effects in different regions may vary among ions. Thus, for a given Cys-loop receptor channel, trying to develop a comprehensive theory to explain all conductance and permeability measurements based on interactions with a single domain in the channel may lead to significant errors. Further, more detailed studies of the interaction of these ions with the cytoplasmic domain will be required to investigate the general applicability of this hypothesis.

Curiously, in the 5-HT3A–glvM3M4–truncated receptors, we observed a negative slope conductance at voltages more negative than −80 mV. A similar negative slope conductance was observed in native receptors. In native 5-HT3A receptors, this was attributed to a voltage-dependent Ca^{2+} block similar to the Mg^{2+} block of NDMA receptors (Van Hooft and Wadman, 2003). However, a recent study in heterologously expressed 5-HT3 receptors suggested that intracellular phosphates may interact with the MA-helix arginine residues, leading to the binding of organic phosphate ions near the cytoplasmic mouth of the channel, thereby facilitating the Ca^{2+} block (Noam et al., 2008). In our experiments, chelation of extracellular Ca^{2+} by EGTA did not affect the negative slope conductance. However, the replacement of the arginine residue in the 5-HT3A–glvM3M4 heptapeptide loop with a glutamine (SQPAQAA) resulted in the loss of the negative slope conductance. Thus, the arginine in the truncated loop may facilitate the localization of complex organic anions in the cytoplasmic mouth of the transmembrane channel, where they can block the pore and inhibit conduction. To account for the voltage dependence of their blocking effects, these anions must be able to interact with the electric field in the channel.

In summary, we conclude that the region that forms the size selectivity filter in 5-HT3 receptors, and probably in other pLGIC superfamily members, is in the cytoplasmic end of the transmembrane channel and not in the portals into the cytoplasmic vestibule. This narrow region of the channel is also the location of the charge selectivity filter. In contrast, the determinants of single-channel conductance are a more distributed property of the protein involving residues along the length of the ion translocation pathway.

We thank Drs. Moez Bali, Alan Finkelstein, Michaela Jansen, and Rishi Parikh for helpful discussions and comments on the manuscript. We thank I.J. Frame and Jarrett Linder for technical assistance.

This work was supported in part by National Institutes of Health (grant NS030808 to M.H. Akabas).

The authors declare no competing interests.

Author contributions: D.C. Reeves and M.H. Akabas designed the experiments; D.C. Reeves and N.K. McKinnon performed the experiments; and D.C. Reeves, N.K. McKinnon, and M.H. Akabas wrote the paper.

Lawrence G. Palmer served as editor.

Submitted: 30 June 2011
Accepted: 6 September 2011

REFERENCES

Akabas, M.H. 2004. $GABA_A$ receptor structure-function studies: a reexamination in light of new acetylcholine receptor structures. *Int. Rev. Neurobiol.* 62:1–43. http://dx.doi.org/10.1016/S0074-7742(04)62001-0

Akabas, M.H., D.A. Stauffer, M. Xu, and A. Karlin. 1992. Acetylcholine receptor channel structure probed in cysteine-substitution mutants. *Science.* 258:307–310. http://dx.doi.org/10.1126/science.1384130

Bali, M., and M.H. Akabas. 2007. The location of a closed channel gate in the $GABA_A$ receptor channel. *J. Gen. Physiol.* 129:145–159. http://dx.doi.org/10.1085/jgp.200609639

Barnes, N.M., T.G. Hales, S.C. Lummis, and J.A. Peters. 2009. The 5-HT3 receptor—the relationship between structure and function. *Neuropharmacology.* 56:273–284. http://dx.doi.org/10.1016/j.neuropharm.2008.08.003

Bera, A.K., M. Chatav, and M.H. Akabas. 2002. GABA(A) receptor M2-M3 loop secondary structure and changes in accessibility during channel gating. *J. Biol. Chem.* 277:43002–43010. http://dx.doi.org/10.1074/jbc.M206321200

Bocquet, N., L. Prado de Carvalho, J. Cartaud, J. Neyton, C. Le Poupon, A. Taly, T. Grutter, J.P. Changeux, and P.J. Corringer. 2007. A prokaryotic proton-gated ion channel from the nicotinic acetylcholine receptor family. *Nature.* 445:116–119. http://dx.doi.org/10.1038/nature05371

Bocquet, N., H. Nury, M. Baaden, C. Le Poupon, J.P. Changeux, M. Delarue, and P.J. Corringer. 2009. X-ray structure of a pentameric ligand-gated ion channel in an apparently open conformation. *Nature.* 457:111–114. http://dx.doi.org/10.1038/nature07462

Brejc, K., W.J. van Dijk, R.V. Klaassen, M. Schuurmans, J. van Der Oost, A.B. Smit, and T.K. Sixma. 2001. Crystal structure of an ACh-binding protein reveals the ligand-binding domain of nicotinic receptors. *Nature.* 411:269–276. http://dx.doi.org/10.1038/35077011

Carland, J.E., M.A. Cooper, S. Sugiharto, H.J. Jeong, T.M. Lewis, P.H. Barry, J.A. Peters, J.J. Lambert, and A.J. Moorhouse. 2009. Characterization of the effects of charged residues in the intracellular loop on ion permeation in alpha1 glycine receptor channels. *J. Biol. Chem.* 284:2023–2030. http://dx.doi.org/10.1074/jbc.M806618200

Changeux, J.P. 2010. Allosteric receptors: from electric organ to cognition. *Annu. Rev. Pharmacol. Toxicol.* 50:1–38. http://dx.doi.org/10.1146/annurev.pharmtox.010909.105741

Cohen, B.N., C. Labarca, N. Davidson, and H.A. Lester. 1992. Mutations in M2 alter the selectivity of the mouse nicotinic acetylcholine receptor for organic and alkali metal cations. *J. Gen. Physiol.* 100:373–400. http://dx.doi.org/10.1085/jgp.100.3.373

Connolly, C.N. 2008. Trafficking of 5-HT(3) and GABA(A) receptors. *Mol. Membr. Biol.* 25:293–301. http://dx.doi.org/10.1080/09687680801898503

Das, P., and G.H. Dillon. 2005. Molecular determinants of picrotoxin inhibition of 5-hydroxytryptamine type 3 receptors. *J. Pharmacol. Exp. Ther.* 314:320–328. http://dx.doi.org/10.1124/jpet.104.080325

Davies, P.A., M. Pistis, M.C. Hanna, J.A. Peters, J.J. Lambert, T.G. Hales, and E.F. Kirkness. 1999. The 5-HT3B subunit is a major determinant of serotonin-receptor function. *Nature.* 397:359–363. http://dx.doi.org/10.1038/16941

Deeb, T.Z., J.E. Carland, M.A. Cooper, M.R. Livesey, J.J. Lambert, J.A. Peters, and T.G. Hales. 2007. Dynamic modification of a mutant cytoplasmic cysteine residue modulates the conductance of the human 5-HT3A receptor. *J. Biol. Chem.* 282:6172–6182. http://dx.doi.org/10.1074/jbc.M607698200

Donizelli, M., M.A. Djite, and N. Le Novère. 2006. LGICdb: a manually curated sequence database after the genomes. *Nucleic Acids Res.* 34:D267–D269. http://dx.doi.org/10.1093/nar/gkj104

Dwyer, T.M., D.J. Adams, and B. Hille. 1980. The permeability of the endplate channel to organic cations in frog muscle. *J. Gen. Physiol.* 75:469–492. http://dx.doi.org/10.1085/jgp.75.5.469

Galzi, J.L., A. Devillers-Thiéry, N. Hussy, S. Bertrand, J.P. Changeux, and D. Bertrand. 1992. Mutations in the channel domain of a neuronal nicotinic receptor convert ion selectivity from cationic to anionic. *Nature.* 359:500–505. http://dx.doi.org/10.1038/359500a0

Goren, E.N., D.C. Reeves, and M.H. Akabas. 2004. Loose protein packing around the extracellular half of the GABA(A) receptor beta1 subunit M2 channel-lining segment. *J. Biol. Chem.* 279:11198–11205. http://dx.doi.org/10.1074/jbc.M314050200

Hales, T.G., J.I. Dunlop, T.Z. Deeb, J.E. Carland, S.P. Kelley, J.J. Lambert, and J.A. Peters. 2006. Common determinants of single channel conductance within the large cytoplasmic loop of 5-hydroxytryptamine type 3 and alpha4beta2 nicotinic acetylcholine receptors. *J. Biol. Chem.* 281:8062–8071. http://dx.doi.org/10.1074/jbc.M513222200

Hansen, S.B., H.L. Wang, P. Taylor, and S.M. Sine. 2008. An ion selectivity filter in the extracellular domain of Cys-loop receptors reveals determinants for ion conductance. *J. Biol. Chem.* 283:36066–36070. http://dx.doi.org/10.1074/jbc.C800194200

Hibbs, R.E., and E. Gouaux. 2011. Principles of activation and permeation in an anion-selective Cys-loop receptor. *Nature.* 474:54–60. http://dx.doi.org/10.1038/nature10139

Hilf, R.J., and R. Dutzler. 2008. X-ray structure of a prokaryotic pentameric ligand-gated ion channel. *Nature.* 452:375–379. http://dx.doi.org/10.1038/nature06717

Hilf, R.J., and R. Dutzler. 2009. Structure of a potentially open state of a proton-activated pentameric ligand-gated ion channel. *Nature.* 457:115–118. http://dx.doi.org/10.1038/nature07461

Horenstein, J., D.A. Wagner, C. Czajkowski, and M.H. Akabas. 2001. Protein mobility and GABA-induced conformational changes in GABA(A) receptor pore-lining M2 segment. *Nat. Neurosci.* 4:477–485.

Hussy, N., W. Lukas, and K.A. Jones. 1994. Functional properties of a cloned 5-hydroxytryptamine ionotropic receptor subunit: comparison with native mouse receptors. *J. Physiol.* 481:311–323.

Imoto, K., C. Busch, B. Sakmann, M. Mishina, T. Konno, J. Nakai, H. Bujo, Y. Mori, K. Fukuda, and S. Numa. 1988. Rings of negatively charged amino acids determine the acetylcholine receptor channel conductance. *Nature.* 335:645–648. http://dx.doi.org/10.1038/335645a0

Jansen, M., M. Bali, and M.H. Akabas. 2008. Modular design of Cys-loop ligand-gated ion channels: functional 5-HT_3 and GABA ρ1 receptors lacking the large cytoplasmic M3M4 loop. *J. Gen. Physiol.* 131:137–146. http://dx.doi.org/10.1085/jgp.200709896

Jones, K.A., and A. Surprenant. 1994. Single channel properties of the 5-HT3 subtype of serotonin receptor in primary cultures of rodent hippocampus. *Neurosci. Lett.* 174:133–136. http://dx.doi.org/10.1016/0304-3940(94)90004-3

Kelley, S.P., J.I. Dunlop, E.F. Kirkness, J.J. Lambert, and J.A. Peters. 2003. A cytoplasmic region determines single-channel conductance in 5-HT3 receptors. *Nature.* 424:321–324. http://dx.doi.org/10.1038/nature01788

Keramidas, A., A.J. Moorhouse, P.R. Schofield, and P.H. Barry. 2004. Ligand-gated ion channels: mechanisms underlying ion selectivity. *Prog. Biophys. Mol. Biol.* 86:161–204. http://dx.doi.org/10.1016/j.pbiomolbio.2003.09.002

Kooyman, A.R., R. Zwart, and H.P. Vijverberg. 1993. Tetraethylammonium ions block 5-HT3 receptor-mediated ion current at the agonist recognition site and prevent desensitization in cultured mouse neuroblastoma cells. *Eur. J. Pharmacol.* 246:247–254. http://dx.doi.org/10.1016/0922-4106(93)90038-B

Kracun, S., P.C. Harkness, A.J. Gibb, and N.S. Millar. 2008. Influence of the M3-M4 intracellular domain upon nicotinic acetylcholine receptor assembly, targeting and function. *Br. J. Pharmacol.* 153:1474–1484. http://dx.doi.org/10.1038/sj.bjp.0707676

Lester, H.A., M.I. Dibas, D.S. Dahan, J.F. Leite, and D.A. Dougherty. 2004. Cys-loop receptors: new twists and turns. *Trends Neurosci.* 27:329–336. http://dx.doi.org/10.1016/j.tins.2004.04.002

Maricq, A.V., A.S. Peterson, A.J. Brake, R.M. Myers, and D. Julius. 1991. Primary structure and functional expression of the 5HT3 receptor, a serotonin-gated ion channel. *Science.* 254:432–437. http://dx.doi.org/10.1126/science.1718042

Noam, Y., W.J. Wadman, and J.A. van Hooft. 2008. On the voltage-dependent Ca2+ block of serotonin 5-HT3 receptors: a critical role of intracellular phosphates. *J. Physiol.* 586:3629–3638. http://dx.doi.org/10.1113/jphysiol.2008.153486

Panicker, S., H. Cruz, C. Arrabit, K.F. Suen, and P.A. Slesinger. 2004. Minimal structural rearrangement of the cytoplasmic pore during activation of the 5-HT3A receptor. *J. Biol. Chem.* 279:28149–28158. http://dx.doi.org/10.1074/jbc.M403545200

Peters, J.A., T.G. Hales, and J.J. Lambert. 2005. Molecular determinants of single-channel conductance and ion selectivity in the Cys-loop family: insights from the 5-HT3 receptor. *Trends Pharmacol. Sci.* 26:587–594. http://dx.doi.org/10.1016/j.tips.2005.09.011

Reeves, D.C., and S.C. Lummis. 2002. The molecular basis of the structure and function of the 5-HT3 receptor: a model ligand-gated ion channel (review). *Mol. Membr. Biol.* 19:11–26. http://dx.doi.org/10.1080/09687680110110048

Reeves, D.C., E.N. Goren, M.H. Akabas, and S.C. Lummis. 2001. Structural and electrostatic properties of the 5-HT3 receptor pore revealed by substituted cysteine accessibility mutagenesis. *J. Biol. Chem.* 276:42035–42042. http://dx.doi.org/10.1074/jbc.M106066200

Tasneem, A., L.M. Iyer, E. Jakobsson, and L. Aravind. 2005. Identification of the prokaryotic ligand-gated ion channels and their implications for the mechanisms and origins of animal Cys-loop ion channels. *Genome Biol.* 6:R4. http://dx.doi.org/10.1186/gb-2004-6-1-r4

Unwin, N. 2005. Refined structure of the nicotinic acetylcholine receptor at 4A resolution. *J. Mol. Biol.* 346:967–989. http://dx.doi.org/10.1016/j.jmb.2004.12.031

Van Hooft, J.A., and W.J. Wadman. 2003. Ca2+ ions block and permeate serotonin 5-HT3 receptor channels in rat hippocampal interneurons. *J. Neurophysiol.* 89:1864–1869. http://dx.doi.org/10.1152/jn.00948.2002

Villarroel, A., S. Herlitze, M. Koenen, and B. Sakmann. 1991. Location of a threonine residue in the alpha-subunit M2 transmembrane segment that determines the ion flow through the acetylcholine receptor channel. *Proc. Biol. Sci.* 243:69–74. http://dx.doi.org/10.1098/rspb.1991.0012

Xu, M., and M.H. Akabas. 1996. Identification of channel-lining residues in the M2 membrane-spanning segment of the $GABA_A$ receptor α_1 subunit. *J. Gen. Physiol.* 107:195–205. http://dx.doi.org/10.1085/jgp.107.2.195

Xu, M., D.F. Covey, and M.H. Akabas. 1995. Interaction of picrotoxin with GABAA receptor channel-lining residues probed in cysteine mutants. *Biophys. J.* 69:1858–1867. http://dx.doi.org/10.1016/S0006-3495(95)80056-1

Yakel, J.L., X.M. Shao, and M.B. Jackson. 1990. The selectivity of the channel coupled to the 5-HT3 receptor. *Brain Res.* 533:46–52. http://dx.doi.org/10.1016/0006-8993(90)91793-G

Yang, J. 1990. Ion permeation through 5-hydroxytryptamine–gated channels in neuroblastoma N18 cells. *J. Gen. Physiol.* 96:1177–1198. http://dx.doi.org/10.1085/jgp.96.6.1177

Yang, J., A. Mathie, and B. Hille. 1992. 5-HT3 receptor channels in dissociated rat superior cervical ganglion neurons. *J. Physiol.* 448:237–256.